ANALYTICA CHIMICA ACTA 614 (2008) 182–189

available at www.sciencedirect.com

ScienceDirect

journal homepage: www.elsevier.com/locate/aca

Label-free cell-based assay using localized surface plasmon resonance biosensor

Tatsuro Endo[a,*], *Shohei Yamamura*[b], *Kagan Kerman*[c], *Eiichi Tamiya*[b,d]

[a] *Department of Mechano-Micro Engineering, Interdisciplinary Graduate of School of Science and Engineering, Tokyo Institute of Technology, 4259 Nagatsuta-cho, Midori-ku, Yokohama 226-8503, Japan*
[b] *Japan Advanced Institute of Science and Technology (JAIST), 1-1 Asahidai, Nomi city, Ishikawa 923-1292, Japan*
[c] *Department of Chemistry, University of Saskatchewan, 110 Science Place, Saskatoon SK S7N 5C9, Canada*
[d] *Department of Applied Physics, Graduate School of Engineering, Osaka University, 2-1 Yamadaoka, Suita, Osaka 565-0871, Japan*

ARTICLE INFO

Article history:
Received 31 December 2007
Received in revised form
7 March 2008
Accepted 11 March 2008
Published on line 15 March 2008

Keywords:
Localized surface plasmon resonance (LSPR)
Biosensor
Cell-based assay
Nanoparticles

ABSTRACT

For an understanding of the life activities, the analysis of cells, which are the smallest units of life form, has a significant impact on biology and biotechnology. In this study, we propose a novel label-free cell-based assay that is based on localized surface plasmon resonance (LSPR) biosensor, which is excited using core–shell structured nanoparticle layer substrate. To demonstrate the promising properties of our LSPR-based label-free cell-based assay, we performed the detection of the cell metabolites using the isolated cells from mouse thymus. For detection of the cellular metabolites, the refractive index change by the specific interaction between the antigen and antibody was detected on the antibody immobilized LSPR-based biosensor. Using our LSPR-based biosensor, the optical characteristics were monitored for the detection of specific reactions between antibody and cell metabolites. As a result, the detection limit of this antibody immobilized LSPR-based biosensor was 10 pg mL^{-1}. Furthermore, the time-course analysis of cell metabolisms using the isolated cells from mouse thymus was also achieved. From these results, the LSPR-based biosensor provides a promising platform with attractive advantages for the detection of biomolecular interactions at low-cost in a simplified experimental set-up with a low sample volume.

1. Introduction

Cells maintain their activities by interacting and functionalizing with each other. Simultaneously, each cell respond with the reception of external stimuli, as a result, the life form can adjust to the external environment and continue its life activities. Furthermore, the cells metabolize in the form of cell metabolites, such as cytokines, for maintaining their life activities. Hence, the detection of the cell metabolites has a critical significance for monitoring the cell activities and functions [1,2]. In addition, the determination of the cell activities and functions has significant applications for several fields, such as environmental monitoring and drug screening [3].

For the determination of the cell activities, a version of enzyme-linked immunosorbent assay (ELISPOT) is widely used as the conventional cell analysis system. ELISPOT is a cell analysis system that count the number of cells, in which the cytokines are secreted, in connection with an antibody [4]. However, the conventional cell analysis systems have several disadvantages, such as troublesome liquid handling, long

* *Corresponding author*. Tel.: +81 45 924 5088; fax: +81 45 924 5088.
E-mail address: endo.t.ab@m.titech.ac.jp (T. Endo).
0003-2670/$ – see front matter © 2008 Elsevier B.V. All rights reserved.
doi:10.1016/j.aca.2008.03.022

assay time and labeling procedure using enzymes and fluorescent dyes. Furthermore, the ELISPOT has limitations for obtaining the quantitative data of the cell metabolite concentrations, since, ELISPOT can only visualize the activities of the cells by counting the "spots" that are generated by the enzymatic reactions on a membrane, such as nitrocellulose and poly(vinylidene fluoride) (PVDF).

On the other hand, the micro-electromechanical systems (MEMS)-based biosensors have become an active area of research for the development of simplified cell-based assay system. Previously, the MEMS-based biosensors utilizing several kinds of detection principles had been reported [5–7]. However, the previously developed MEMS-based biosensors for cell-based assay require a labeling procedure for the determination of cell activities. Hence, a novel biosensor with a novel detection principle for the label-free determination of cell activities and functions is still highly desired.

To overcome these disadvantages of conventional cell analysis systems and MEMS-based biosensors, we focused on the unique characteristics of the nanostructured materials, such as nanoparticles. The rapid development of nanotechnology and nanostructured materials brought along a novel and exciting field of research. Furthermore, the inherently small size and unusual optical, magnetic, catalytic and mechanical properties of nanoparticles not found in bulk materials provided a strong platform for the development of novel devices and applications in electronics, optics and biotechnology [8–10]. Therefore, the characteristics of the nanomaterials, such as nanoparticles, nanotubes and nanofibers have been studied in detail [11–13]. The nanostructured materials possess well-defined optical characteristics due to their quantum size effects. In addition, they are sensitive to the surrounding environmental changes, such as refractive index. This property of nanoparticles enabled the label-free detection of cell metabolites using our biosensor.

Until now, we achieved the label-free detection of the bimolecular interactions, such as antigen–antibody reactions, DNA–DNA and peptide nucleic acid (PNA)–DNA hybridizations [14–18] using localized surface plasmon resonance (LSPR)-based biosensor. As a result, we have established a highly sensitive method for the label-free detection of the biomolecular interactions. LSPR is one of the specific characteristics of metallic or metallized nanostructured materials, such as noble metal nanoparticles [19]. Especially, Au and Ag nanoparticles are subject to active research because of their well-documented or proposed importance in various nano-optical applications, such as biosensors [20–23], and even a nanoruler [24]. The LSPR-based biosensor can detect an immediate increase in the thickness of a biomolecular layer on the surface of a sensitive element caused by the reaction between the solution component under study and the receptor layer immobilized on the surface. Using these characteristics, our LSPR-based biosensor was applied to label-free detection of the cellular metabolism reactions. In our previous reports, we achieved the applicability of this LSPR-based biosensor by using proteins, DNA and PNA as the target molecules. Since cells are applied to the LSPR-based biosensor in this report, we demonstrate that the applicability of this biosensor can be more defined in a wide range of fields, such as medical, food control, environmental monitoring and drug screening.

For the evaluation of LSPR-based biosensor for label-free cell assay in this study, label-free detection of the interleukin-2 (IL-2) from mouse cells as a model case was carried out. IL-2 is the primary T cell growth factor secreted by the activated T cells [25,26]. IL-2 is an α-helical cytokine that binds to a multi subunit receptor expressed on the surface of a variety of cell types. Hence, monitoring IL-2 from living cells without labeling procedure can be applicable to monitor the other cell metabolites. The application of our LSPR-based biosensor for label-free cell analysis provided a more convenient analysis system than the conventional ELISPOT. In parallel, the conventional cell-based assays, such as ELISA and ELISPOT were also carried out for comparison of the characteristics of our LSPR-based biosensor.

2. Experimental

2.1. Materials

For the self-assembled monolayer (SAM) formation on the gold substrate surface, 4,4′-dithiodibutyric acid (DDA) was purchased from Aldrich. For the activation of the carboxyl group of DDA, 1-ethyl-3-(3-dimethylaminopropyl)carbodiimide (EDC) was purchased from Dojindo Laboratories (Kumamoto, Japan). 3-Aminopropyltriethoxysilane (γ-APTES) for surface modification of silica nanoparticles was purchased from Shin-Etsu Chemical Co., Ltd. (Tokyo, Japan). Silica nanoparticles (100 nm i.d.) for preparing the nanoparticle layer were purchased from Polysciences Inc. (Warrington, PA). Slide glass substrate (S-1111, 76 mm × 26 mm, thickness: 0.8–1.0 mm) was purchased from Matsunami Glass Ind. Ltd. (Osaka, Japan). Electronic grade of sulfonic acid and hydrogen peroxide for cleaning the slide glass substrate were purchased from Kanto Kagaku (Tokyo, Japan). *N*-Hydroxysuccinimide (NHS) for antibody immobilization was purchased from Wako Pure Chemical Industries, Ltd. (Osaka, Japan). The monoclonal anti-mouse IL-2 antibody (MAB702, R&D Systems, Inc.) and antigen (IL-2 recombinant, Mouse Expressed in *Escherichia coli*, I0523) were obtained from Cosmo Bio (Tokyo, Japan). Ultra-pure water (18.3 MΩ cm) from Millipore was used in all preparations. In addition, to compare the characteristics of our biosensor, conventional ELISA kit (KMC0021, BioSource International, Inc.) and ELISPOT kit (DSM001-1, Euroclone) were obtained.

2.2. Apparatus

For the deposition of gold and chromium layer on the slide glass substrate, a thermal evaporator (SVC-700TM/700-2) was purchased from Sanyu Electron Co., Ltd. (Tokyo, Japan). For monitoring of the base pressure, an analog Ionization Vacuum Gauge was utilized (GI-TL3, ULVAC, Kanagawa, Japan). The growth rate in thickness was monitored by a quartz crystal microbalance (QCM, Model TM-200R, MAXTEK. Inc., CA, USA). Spectrophotometer (USB-2000-UV–vis, wavelength range: 200–1100 nm), tungsten halogen light source (LS-1, wavelength range: 360–2000 nm) and optical fiber probe bun-

dle (R-200-7 UV–vis, fiber core diameter: 200 μm, wavelength range: 250–800 nm) for evaluation of the optical characteristics of LSPR-based biosensor, were purchased from Ocean Optics (Dunedin, USA).

2.3. *Fabrication of LSPR-based biosensor for label-free cell based assay*

Our LSPR-based biosensor was constructed by a core–shell structured nanoparticle layer (Fig. 1a), the surface modified silica nanoparticle was used as the "core", and the "shell" was applied with a gold layer that was deposited onto the core surface using thermal deposition.

For the preparation of the surface modified silica nanoparticles, silica nanoparticles (particle diameter: 100 nm) were dried over 24 h at 55 °C, and reacted with 1% (v/v) 3-aminopropyltriethoxysilane (γ-APTES) solution in ultra pure water for 24 h at room temperature (RT) by stirring continuously. After the surface modification, the γ-APTES solution was removed in the centrifugal operation for 1 h at 3500 rpm and the centrifuged surface modified silica nanoparticles were washed with ultra pure water. Both of the washing and centrifugal operations were repeated for three times. After these operations, surface modified nanoparticles were dried up for 5 min at 120 °C. Silica nanoparticles modified with amino groups were thus obtained. Finally, surface modified nanoparticles were stored in the desiccator before use. Then, the surface modified silica nanoparticles colloid solution was prepared by dispersing in ultra pure water for the formation of the nanoparticle layer.

After the pretreatment of their surfaces, slide glasses were used as substrates for the formation of the nanoparticle layer. All substrates were cleaned via a three-step process of ultrasonic cleaning in acetone for 30 min, soaking in sulfuric acid and hydrogen peroxide solution (Piranha solution) at a ratio of 5:1 (v/v) for 30 min, followed by thorough rinsing with ultrapure water, and drying at RT. Finally, they were stored in the desiccator before use. *Caution*: Piranha solution is corrosive. In addition, care should be taken not to store piranha solution for extended periods of time because of the formation of explosive oxides.

For the fabrication of LSPR-based biosensor using surface modified silica nanoparticles, 1 mM of DDA solution was introduced to the gold-deposited slide glass substrate

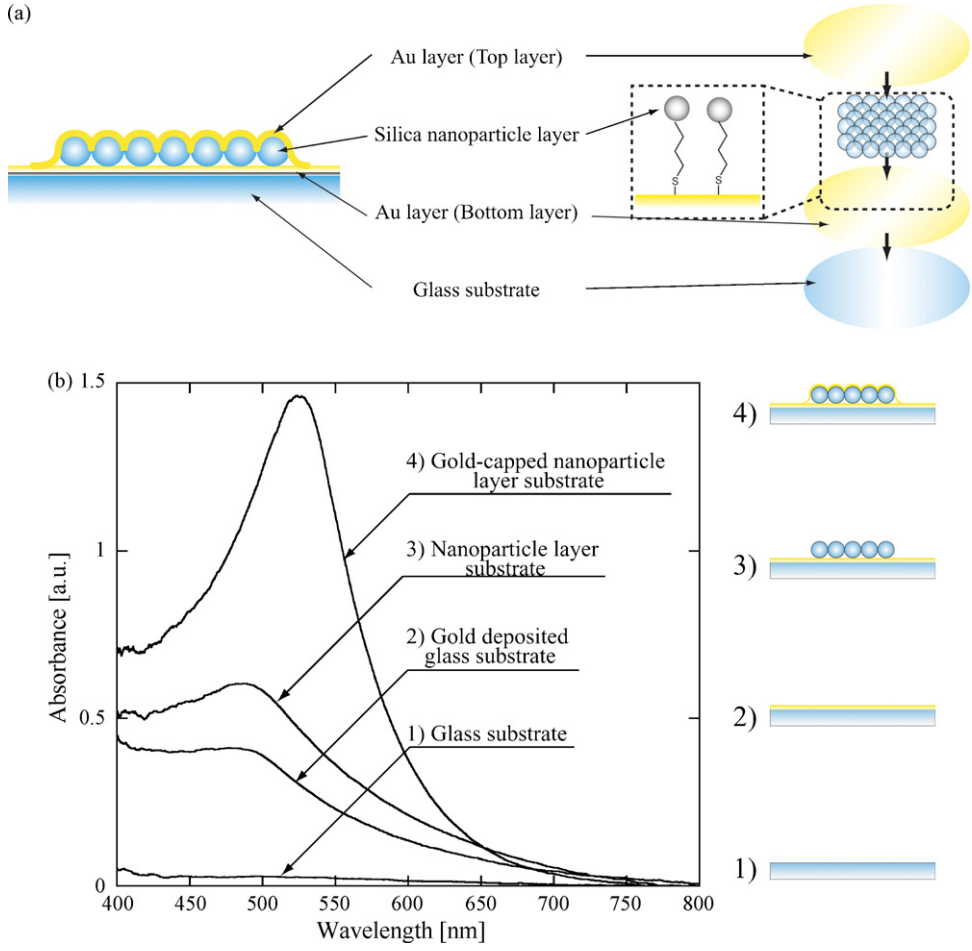

Fig. 1 – (a) Construction of LSPR-based label-free biosensor. The surface modified silica nanoparticles layer was formed on the Au-deposited glass substrate surface. Furthermore, the Au layer was formed on the nanoparticle layer using thermal evaporation. (b) Optical characteristics of the gold-capped nanoparticle layer substrate. Specific LSPR absorbance peak was observed with only the gold-capped nanoparticle layer substrate.

surface produced by the thermal evaporation and the self-assembled monolayer (SAM) was formed in 1 h. The SAM-functionalization was carried out with 400 mM EDC solution for 1 h, EDC activated the carboxyl groups of the DDA, and therefore, the amino groups of silica nanoparticles could form esters with the activated carboxyl groups. The surface modified silica nanoparticles that were modified with amino groups (1%, w/v) by silane coupling reagent in ultra pure water, were exposed to the activated SAM modified gold substrate surface for 1 h. The nanoparticle layer modified substrates were rinsed thoroughly with ultrapure water to remove the excess surface modified nanoparticles, and dried at RT. While the preparation of the nanoparticle layer, the silicon rubber sheet was attached on the gold layer deposited slide glass substrate surface for hold sample solutions to form the nanoparticle layer. The uniformly sized nanoparticle layer could be formed with the help of a silicon rubber sheet that supported the nanoparticle layer. Finally, gold layer (30 nm) was deposited on the nanoparticle layer modified substrates using thermal evaporator (Fig. 1a). After these fabrication procedures, the LSPR band was monitored in the visible range. As a result, the core–shell structured nanoparticle layer substrate for LSPR excitation could be obtained (Fig. 1b).

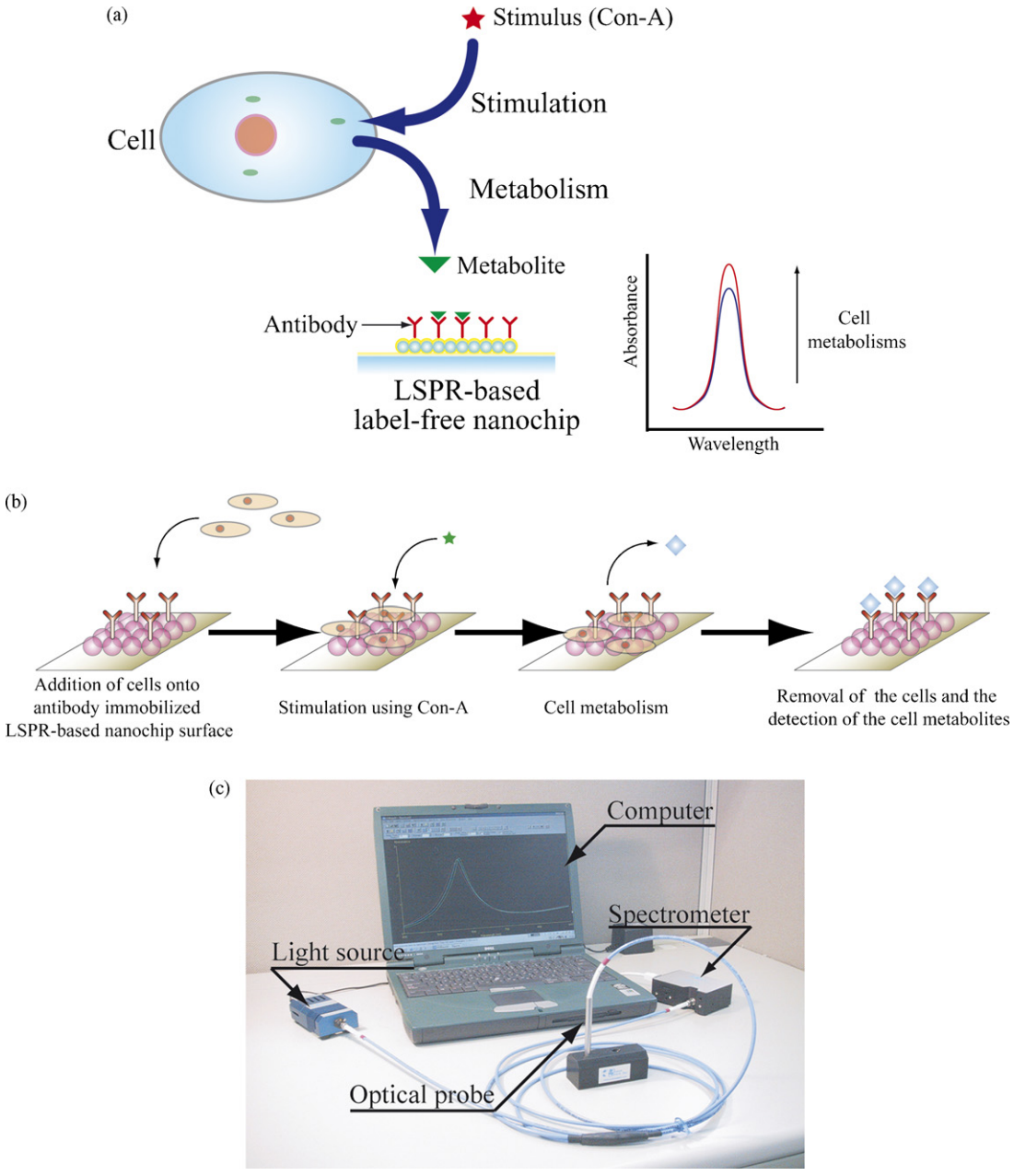

Fig. 2 – (a) Schematic illustration of label-free cell analysis system. The antibody immobilized LSPR-based label-free biosensor was applied to detect the cell metabolites, such as cytokines. (b) Experimental procedure using label-free cell analysis system. (c) Optical characteristics of the gold-capped nanoparticle layer substrate. Specific LSPR absorbance peak was observed with only the gold-capped nanoparticle layer substrate.

In addition, for the evaporation, the thermal evaporator was used at a base pressure of 8×10^{-6} Torr; the growth rate was monitored by a QCM, and manually adjusted to 1.0 Å s^{-1}. Gold and chromium of 99.99% purity was obtained from Furuya Metal (Tokyo, Japan). A chromium layer of 5 nm and a gold layer of 40 nm were deposited onto the glass substrates. Furthermore, after the formation of the nanoparticle layer, 30 nm of the gold layer was deposited onto the formed nanoparticle layer using the surface-modified silica nanoparticles for the LSPR-based biosensor fabrication.

2.4. *Immobilization of antibodies onto the LSPR-based biosensor surface*

The antibody immobilization was carried out with an almost similar procedure to the formation of nanoparticle layer onto gold-deposited slide glass substrate surface using surface modified silica nanoparticles. DDA solution of 1 mM was introduced to the LSPR-based biosensor surface, and SAM was formed in 1 h. The SAM-functionalization was carried out using 400 mM EDC for 1 h, and then 100 mM NHS was added to the SAM-functionalized LSPR-based biosensor surface for 1 h. Protein A at 100 μg mL^{-1} was introduced to the LSPR-based biosensor surface for 1 h, which enabled the binding with the Fc region of the IgG antibody, therefore the conformation of the antibody became possible to control. Anti-IL-2 antibody at 100 μg mL^{-1} was introduced to the protein A modified surface for 1 h. The immobilization of the antibody was achieved after these steps. Finally, the antibody immobilized LSPR-based biosensor surface was rinsed thoroughly with 20 mM phosphate buffered saline (PBS, pH 7.4) and dried at RT.

In addition, for the evaluation of the characteristics using antibody immobilized LSPR-based biosensor, the selection of the substrate, which has similar LSPR optical characteristics and nanoparticle coverage was also carried out. For the selection of substrates, optical characterization of the LSPR absorbance strength and the peak wavelength, as well as atomic force microscopy (AFM) for the evaluation of nanoparticle coverage were performed.

2.5. *Application for label-free cell-based assay using antibody immobilized LSPR-based biosensor*

Fig. 2b shows the experimental procedure of label-free cell-based assay using antibody immobilized LSPR-based biosensor. After the immobilization of the antibody, serial dilutions of IL-2 (0–100 μg mL^{-1}) were introduced to the antibody immobilized LSPR-based biosensor for evaluation of the calibration characteristics, and the change in the absorption spectrum caused by the antibody–antigen reaction was observed. Using the calibration characteristics, the isolated cells from mouse thymus was applied to detect the cell metabolites using antibody immobilized LSPR-based biosensor.

For the detection of the cell metabolites, the isolated cells (1×10^3 and 1×10^6 cells mL^{-1}) with 20 mM PBS buffer were introduced to the antibody immobilized LSPR-based biosensor. For stimulation of the cells, the stimulus (1.0 μg mL^{-1} of Con-A) was introduced to the cells. The stimulated cells were incubated at 37 °C. After the stimulation using Con-A, observation of the absorbance intensity changes caused by the IL-2 metabolism was carried out at various incubation periods. In addition, the evaluation of LSPR optical characteristics was carried out after washing the biosensor surface with 20 mM PBS buffer and drying up at RT.

3. Results and discussion

3.1. *Calibration characteristics of the antibody immobilized LSPR-based biosensor*

Anti mouse IL-2 antibody was immobilized on LSPR-based biosensor surface for the specific determination of IL-2 concentration from mouse cells. After the immobilization of anti-IL-2 antibody onto LSPR-based biosensor surface, the calibration characteristics of this LSPR-based biosensor were monitored. For the evaluation of characteristics, serial dilutions of IL-2 solutions were introduced to the antibody

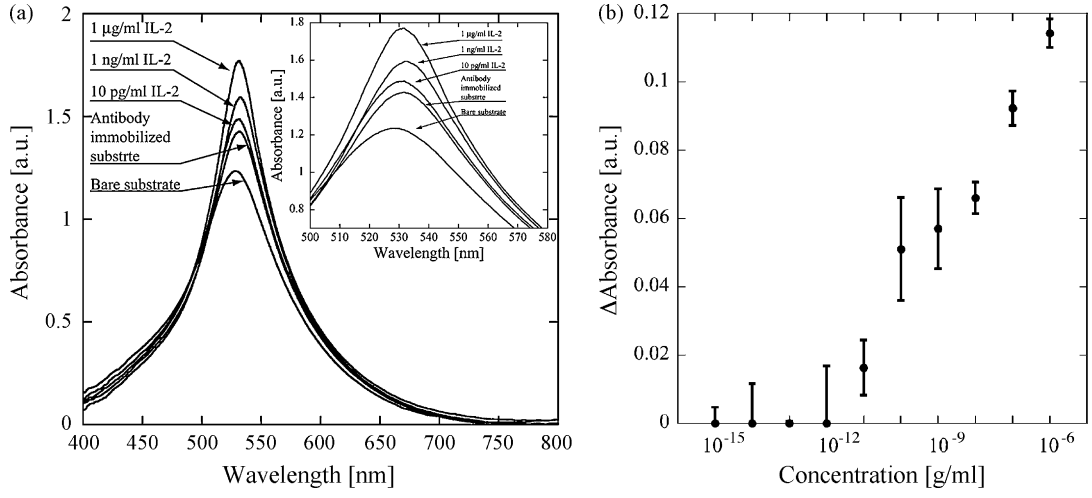

Fig. 3 – (a) LSPR absorbance strength changes with antigen concentrations. (b) Calibration characteristics of the antibody immobilized LSPR-based label-free biosensor. The detection limit of this biosensor was 10 pg mL^{-1}. Based on these characteristics, the determination of IL-2 metabolism was carried out.

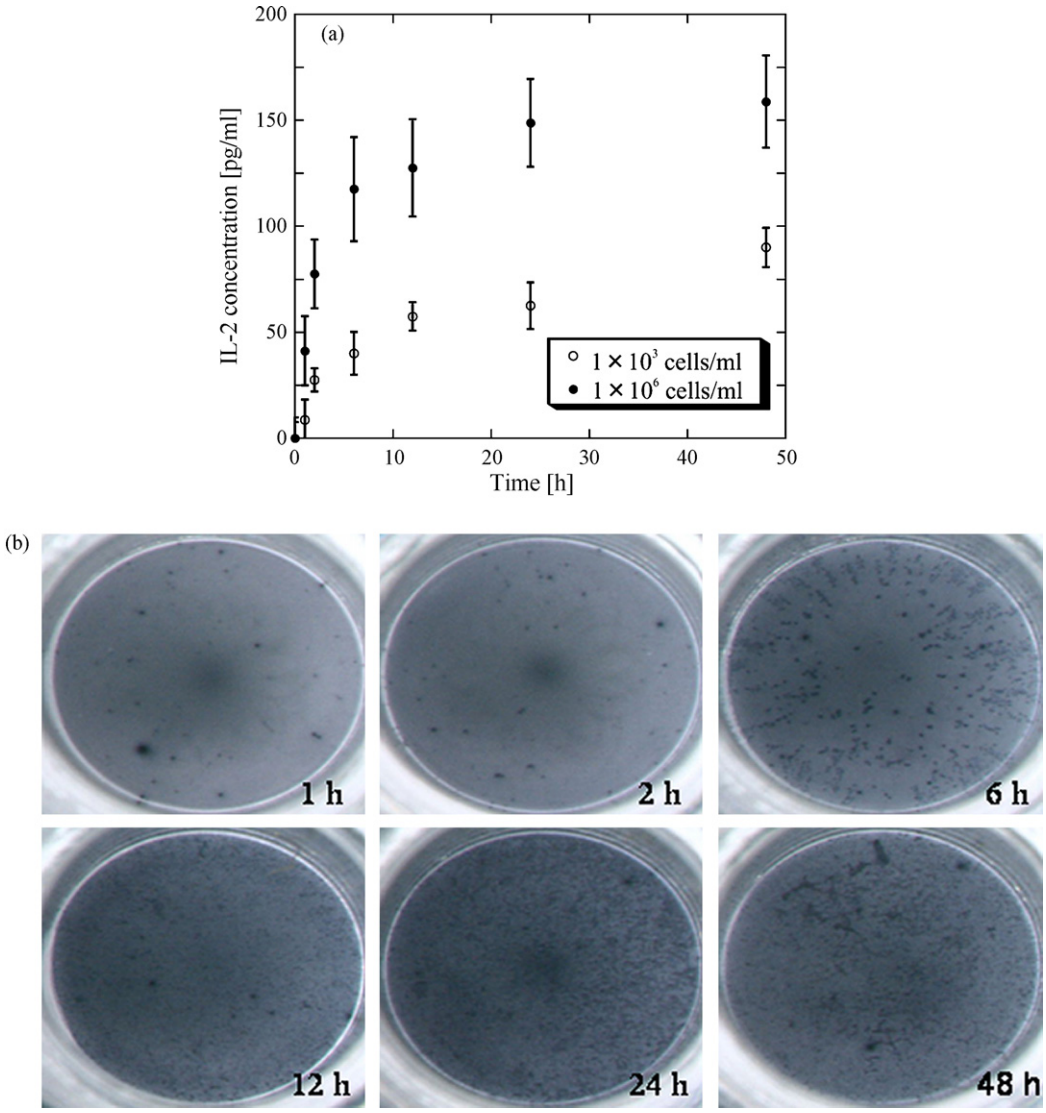

Fig. 4 – (a) Incubation time dependency using LSPR-based label-free cell analysis system. After the stimulation using Con-A, the absorbance intensity increments caused by the IL-2 metabolism was observed. (b) Observation of the cell metabolism using ELISPOT. The "spots" caused by the cell metabolism depending on the incubation time was observed. However, the ELISPOT assay does not provide quantitative information about the concentration of IL-2 based on the appearance of the "spots". Therefore, our label-free cell analysis system enables significant advantages to the conventional cell analysis systems.

immobilized LSPR-based biosensor surface. From these introducing procedures, the response was proportional to the concentration only on a half-logarithmic scale. After the introduction of the IL-2 solutions (0–100 $\mu g\,mL^{-1}$), optical characteristics evaluation was carried out (Fig. 2a and b). In this study, all absorbance spectra were taken from 400 to 800 nm on the UV–vis spectrometer at room temperature. White light emerging from the optical fiber bundle was incident onto the LSPR-based biosensor from the vertical direction. The reflected light was coupled into the detection fiber probe of the same optical fiber bundle and analyzed by the UV–vis spectrometer. Using this experimental set-up, the measurement system became portable and significantly smaller than the conventional SPR system (Fig. 2c). The LSPR optical characteristics changed with the antigen concentrations as shown in Fig. 3a. Using anti-IL-2 antibody immobilized LSPR-based biosensor, the specific absorbance intensity increments depending on IL-2 concentration could be observed (detection limit: 10 $pg\,mL^{-1}$, Fig. 3b). Based on the success of immunological recognition results, this antibody immobilized LSPR-based biosensor was applied for label-free cell analysis system. In addition, when the 100 $\mu g\,mL^{-1}$ of bovine serum albumin (BSA) solution was introduced onto the anti-IL-2 antibody immobilized LSPR-based biosensor as a negative control, the fractional absorbance intensity increments (approximately 0.01 a.u.) by the non-specific adsorption could be observed. In this study, for the evaluation of calibration characteristics, the intensity increments by the non-specific adsorption were subtracted as a background.

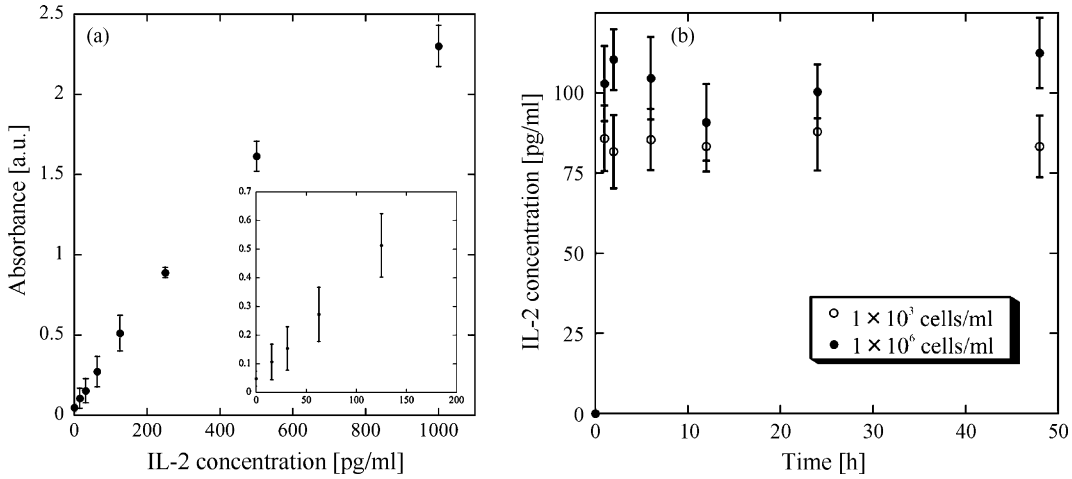

Fig. 5 – (a) Calibration characteristics of the conventional ELISA for IL-2. (b) Incubation time dependency using conventional ELISA. Using ELISA, the quantitative determination of the IL-2 from mouse cells, and almost similar behavior of IL-2 metabolism and concentration could be observed with the similar calibration plot characteristics.

3.2. *Time-course analysis of the cell metabolisms using LSPR-based biosensor*

For application of label-free cell analysis system using antibody immobilized LSPR-based biosensor, the isolated cells from the thymus of a 6-week-old male mouse were used. Serial dilutions of the isolated cells (1×10^3 and 1×10^6 cells mL^{-1}) were introduced onto the antibody immobilized LSPR-based biosensor surfaces. For the stimulation of the cells, concanavalin-A (con-A) was applied. Con-A is a glycoprotein that promotes mitosis and stimulates T lymphocytes. Therefore, its expression triggered the secretion of IL-2 [27]. Con-A solution (1.0 $\mu g\,mL^{-1}$) was introduced to the each cell modified biosensor surface at time zero. Furthermore, the incubation was stopped at each incubation time (1, 2, 6, 12, 24 and 48 h). After the incubation, LSPR-based biosensor surfaces were washed with 20 mM PBS, and the surfaces were dried up at RT. From these experimental procedures, optical characteristics evaluation was carried out. Furthermore, the metabolized IL-2 concentration from mouse cells was determined from calibration plots. In addition, the conventional cell analysis system, ELISPOT was also carried out to compare with the characteristics of the cell metabolism on our biosensor.

As a result of determination of cell metabolism using the antibody immobilized LSPR-based biosensor, the absorbance strength change depending on the incubation time and cell concentration could be observed (Fig. 4a). The increments in the absorbance intensity were observed immediately after the application of the stimuli. From these characteristics, we determined that 75–150 pg mL^{-1} and of IL-2 was metabolized as a result of con-A stimulation. In addition, without the stimulation using Con-A and anti-dinitrophenylated bovine serum albumin (DNP-BSA) antibody immobilized LSPR-based biosensor was applied to similar experiment as a negative control; we could not observe any significant absorbance strength change (approximately 0.05–0.01 a.u.; data not shown).

Simultaneously, the comparison of the characteristics between LSPR-based biosensor and the conventional cell analysis system ELISPOT was carried out. In addition, the cell analysis using ELISPOT, we could observed that the trend of cell activity. However, using ELISPOT, the quantitative determination of IL-2 concentration from mouse cells is a difficult task (Fig. 4b). On the other hand, for comparison of the characteristics of this LSPR-based optical biosensor for label-free cell assay, conventional ELISA was carried out. Using ELISA, the quantitative determination of the IL-2 from mouse cells, and almost similar behavior of IL-2 metabolism and concentration could be observed with the similar calibration plot characteristics (Fig. 5a and b).

From these results, we suggest that using our antibody immobilized LSPR-based biosensor has a great potential in applications in the high-throughput cell analysis systems for monitoring of cell activities and functions.

4. Conclusions

The novel cell analysis system using LSPR-based biosensor enables user friendly, convenient, detection of cell metabolites with high specificity and sensitivity at a low-cost, because there is no necessity of labeling procedure on this monitoring method. In addition, this LSPR-based biosensor and the measurement apparatus cost is lower than that of conventional SPR apparatus, and the operation procedure is more convenient and easy. Therefore, this LSPR-based biosensor has flexibility for analyzing various kinds of biomolecular interactions on the chip surface.

Acknowledgements

The authors wish to thank Dr. Yasuko Yanagida and Dr. Takeshi Hatsuzawa from the Tokyo Institute of Technology (Tokyo Tech.) and Dr. Naoki Nagatani from the Okayama University of Science for useful suggestions during the preparation of this manuscript.This study was supported by

the JST-SENTAN program (System Development Program for Advanced Measurement and Analysis) of Japan Science and Technology Agency (JST).

REFERENCES

[1] M.A. Cooper, Nat. Rev. Drug Discov. 1 (2002) 515.
[2] T. Kaletta, M.O. Hengartner, Nat. Rev. Drug Discov. 5 (2006) 387.
[3] J.R. Soglia, S.P. Harriman, S. Zhao, J. Barberia, M.J. Cole, J.G. Boyd, L.G. Contillo, J. Pharm. Biomed. Anal. 36 (2004) 105.
[4] D.D. Anthony, P.V. Lehmann, Methods 29 (2003) 260.
[5] X. Feng, J. Castracane, N. Tokranova, A. Gracias, G. Lnenicka, B.G. Szaro, Biosens. Bioelectron. 22 (2007) 3230.
[6] S. Bouaidat, C. Berendsen, P. Thomsen, S.G. Petersen, A. Wolff, J. Jonsmann, Lab Chip 4 (2004) 632.
[7] C.H. Tai, S.K. Hsiung, C.Y. Chen, M.L. Tsai, G.B. Lee, Biomed. Microdevices 9 (2007) 533.
[8] A.J. Haes, R.P. Van Duyne, Anal. Bioanal. Chem. 379 (2004) 920.
[9] N. Nath, A. Chilkoti, Anal. Chem. 74 (2002) 504.
[10] C.R. Yonzon, E. Jeoung, S. Zou, G.C. Schatz, M. Mrksich, R.P. Van Duyne, J. Am. Chem. Soc. 126 (2004) 12669.
[11] P.N. Prasad, Nanophotonics, John Wiley & Sons., Hoboken, New Jersey, USA, 2004.
[12] G. Mie, Annalen der Physik 25 (1908) 377.
[13] R. Jin, Y. Cao, C.A. Mirkin, K.L. Kelly, G.C. Schatz, J.G. Zheng, Science 294 (2001) 1901.
[14] T. Endo, S. Yamamura, N. Nagatani, Y. Morita, Y. Takamura, E. Tamiya, Sci. Tech. Adv. Mater. 6 (2005) 491.
[15] T. Endo, K. Kerman, N. Nagatani, Y. Takamura, E. Tamiya, Anal. Chem. 77 (2005) 6976.
[16] T. Endo, K. Kerman, N. Nagatani, H.M. Hiep, D.-K. Kim, Y. Yonezawa, K. Nakano, E. Tamiya, Anal. Chem. 78 (2006) 6465.
[17] T. Endo, K. Kerman, N. Nagatani, E. Tamiya, J. Phys. Condens. Matter 19 (2007) 215201.
[18] H.M. Ha, T. Endo, K. Kerman, M. Chikae, D.-K. Kim, S. Yamamura, Y. Takamura, E. Tamiya, Sci. Tech. Adv. Mater. 8 (2007) 331.
[19] A.J. Haes, R.P. Van Duyne, J. Am. Chem. Soc. 124 (2002) 10596.
[20] P. Mulvaney, Langmuir 12 (1996) 788.
[21] D.A. Stuart, C.R. Yonzon, X. Zhang, O. Lyandres, N.C. Shah, M.R. Glucksberg, J.T. Walsh, R.P. Van Duyne, Anal. Chem. 77 (2005) 4013.
[22] C. Sönnichsen, B.M. Reinhard, J. Liphardt, A.P. Alivisatos, Nat. Biotechnol. 23 (2005) 741.
[23] A.J. Haes, L. Chang, W.L. Klein, R.P. Van Duyne, J. Am. Chem. Soc. 127 (2005) 2264.
[24] M. Himmelhaus, H. Takei, Sensors Actuat. B 63 (2000) 24.
[25] S.L. Gaffen, Cytokine 14 (2001) 63.
[26] S. Boulet, M.L. Ndongala, Y. Peretz, M.P. Boisvert, M.R. Boulassel, C. Tremblay, J.P. Routy, R.P. Sekaly, N.F. Bernard, J. Immunol. Methods 320 (2007) 18.
[27] P. Dráber, Int. J. Immunopharmacol. 4 (1982) 401.